Original Article
Adipose-derived mesenchymal stem cell-derived exosomes markedly protected the brain against sepsis syndrome induced injury in rat

Chia-Lo Chang[1*], Hong-Hwa Chen[1], Kuan-Hung Chen[2], John Y Chiang[5,6], Yi-Chen Li[3], Hung-Sheng Lin[4], Pei-Hsun Sung[3], Hon-Kan Yip[3,7,8,9,10*]

[1]Division of Colorectal Surgery, Department of Surgery, [2]Department of Anesthesiology, [3]Division of Cardiology, Department of Internal Medicine, [4]Division of Neurology, Department of Internal Medicine, Kaohsiung Chang Gung Memorial Hospital and Chang Gung University College of Medicine, Kaohsiung 83301, Taiwan; [5]Department of Computer Science and Engineering, National Sun Yat-Sen University, Kaohsiung, Taiwan; [6]Department of Healthcare Administration and Medical Informatics, Kaohsiung Medical University, Kaohsiung, Taiwan; [7]Institute for Translational Research in Biomedicine, [8]Center for Shockwave Medicine and Tissue Engineering, Kaohsiung Chang Gung Memorial Hospital, Kaohsiung 83301, Taiwan; [9]Department of Medical Research, China Medical University Hospital, China Medical University, Taichung 40402, Taiwan; [10]Department of Nursing, Asia University, Taichung 41354, Taiwan. *Equal contributors.

Abstract: This study tested the hypothesis that sepsis syndrome [SS-induced by cecal-ligation and puncture (CLP)]-induced systemic inflammation and brain damage in rats were effectively suppressed by allogenic adipose-derived mesenchymal stem cell-derived exosome (AMSC^{EXO}). SD rats (n = 72) were divided into group 1 [sham-control (SC)], group 2 (SS only) and group 3 (SS + AMSC^{EXO}) and equally euthanized at 6/24/48/72 h after SS induction, respectively. By 6/16/24/72 h, flow cytometric analyses demonstrated the numbers of inflammatory cells (Ly6G+/CD11$^{b/}$^{c}+), immune (CD3+/CD4+ cells/CD3+/CD8+ cells) and early (AN-V+/PI-)/late (AN-V+/PI+) apoptotic cells in circulation were significantly increased in group 2 than in groups 1 and 3, and significantly increased in group 3 than in group 1, whereas the number of T-reg+ cells was significantly progressively increased from groups 1 to 3 (all P < 0.0001). At 6/16/24/72 h, the numbers of (CD3+/CD4+ cells/CD3+/CD8+ cells/T-reg+ cells) in spleen exhibited an identical pattern of circulation among the three groups (all P < 0.0001). ELISA showed inflammatory mediators (IL-6/TNF-α) in circulating/cerebrospinal fluid at 6/24/72 h displayed an identical trend as the immune cells among the three groups (all P < 0.0001). Microscopic findings demonstrated that the cellular expressions of inflammatory (F4/80+//MMP-9+//CD14+//GFPA+) and brain-damaged (AQP4+/γ-H2AX+) biomarkers at 24/72 h exhibited an identical pattern of immune cells among the three groups (all P < 0.0001). The protein expressions of inflammatory (IL-1β/MMP-9/TNF-α/NF-κB/TLR2/TLR-4/MyD88/HMGB1), apoptotic (cleaved-caspase3/PARP/mitochondrial-Bax) and oxidative-stress (NOX-1/NOX-2/oxidized protein) biomarkers displayed an identical pattern as the immune cells among the three groups (all P < 0.0001). In conclusion, SS elicited vigorously inflammatory reaction not only in circulation but also in spleen/brain, resulting in serious brain damage.

Keywords: Sepsis syndrome, inflammation, oxidative stress, apoptosis, brain damage

Introduction

Sepsis syndrome (SS), characterized by systemic inflammatory reaction caused by infection, is a very common public health issue with an extremely high economic burden through health care costs worldwide [1-3]. Abundant data have shown that SS is still the major leading cause of death in ICU, ranging from 20% in sepsis to more than 60% in SS complicated by septic shock [1-8]. Although utilization of ad-

vanced antibiotics is the golden standard method for treatment of SS [1, 2, 9, 10], the in-hospital morbidity and mortality rates of SS remain unacceptably high, highlighting that there is an urgent need for innovative and efficacious therapies for treatment.

Undoubtedly, severe sepsis frequently causes multiple organ failure [8, 10-12]. Of these major organs, brain is not only commonly involved but also one of the most vulnerable organs subject-

ed to serious damage via metabolic or inflammatory disturbances. In fact, neurologic complications, such as sepsis-associated encephalopathy, frequently occur early in septic patients and are associated with even higher mortality and long-term complications such as cognitive dysfunction [13-18]. Studies have further demonstrated that septic encephalopathy and polyneuropathy occur in 70% of septic patients [13]. Interestingly, despite the incidence of SS-associated central nervous system (CNS) complication and relevant prognosis are clear; however, the underlying mechanisms remain a heatedly debated issue [14-18].

Previous studies have exhibited that host's defense mechanisms, including uncontrolled overwhelming inflammatory response and hyperactivity of immune system in response to infectious stimulation along with complement cascade which not only fight against bacterial infection but also attack and damage the host's organs, are the major contributors of high mortality in SS patients [9, 18-22]. Interestingly, some studies have revealed that systemic inflammation appears to play a key role in both altering the blood-brain barrier permeability and amplifying the inflammatory response [15]. These aforementioned issues [9, 15, 18-22] raised the hypothesis that early targeting on the inflammatory signaling might have a potentially therapeutic impact on protecting the brain organ failure against SS.

Intriguingly, plentiful studies have shown that the mesenchymal stem cell (MSC)-derived exosomes which have capacities of angiogenesis, immunomodulation, anti-inflammation and the paracrine effect protect the organ function following injury in preclinical studies [23-28]. Our previous studies [15, 24, 29, 30] have shown that adipose-derived MSC (i.e., ADMSC)-derived exosomes effectively protected the organs from sepsis or ischemia-reperfusion damage mainly through regulating the inflammatory-oxidative signaling axis. Accordingly, we proposed that ADMSC-derived exosomes might have therapeutic benefit on protecting the brain organ from SS induced injury.

Materials and methods

Ethics

All animal procedures were approved by the Institute of Animal Care and Use Committee at Kaohsiung Chang Gung Memorial Hospital (Affidavit of Approval of Animal Use Protocol No. 2016032201) and performed in accordance with the Guide for the Care and Use of Laboratory Animals.

Animals were housed in an Association for Assessment and Accreditation of Laboratory Animal Care International (AAALAC; Frederick, MD, USA)-approved animal facility in our hospital with controlled temperature and light cycles (24°C and 12/12 light cycle).

Procedure for SS induction by cecal ligation and puncture (CLP)

The procedure and protocol of SS induction have been described in our previous reports [11, 12, 31]. In detail, Pathogen-free, adult male Sprague-Dawley (SD) rats weighing 320-350 g (Charles River Technology, BioLASCO, Taiwan) were utilized in the present study. Rats were anesthetized with inhalational 2.0% isoflurane and placed supine on a warming pad at 37°C with the abdomen shaved. Under sterile conditions, the abdominal skin and muscle were opened and the cecum exposed in all groups. In the sham-control animals, the abdomen was then closed and the animal was allowed to recover from anesthesia. In the experimental CLP groups, the cecum was ligated with prolene suture over its distal portion (i.e., distal ligation) and the cecum distal to the ligature was punctured twice with an 18# needle to allow the cecal contents to be expressed intraperitoneally, as previously described [11, 12, 31]. The wound was closed and the animal was allowed to recover from anesthesia.

Isolation of ADMSCs

For preparation of allogenic ADMSCs, additional 20 SD rats were utilized in the present study. Adipose tissue surrounding the epididymis was dissected, excised and prepared based on our recent reports [11, 12, 31]. Briefly, the tissue was carefully cut into pieces < 1 mm³ using a pair of sharp, sterile surgical scissors. Sterile saline (37°C) was added to the homogenized adipose tissue in a ratio of 3:1 (saline: adipose tissue), followed by the addition of stock collagenase solution to a final concentration of 0.5 units/mL. The centrifuge tubes with the contents were placed and secured on a Thermaline shaker and incubated with constant agitation

for 60 minutes at 37°C. After 40-45 minutes of incubation, the contents were triturated with a 25-mL pipette for 3 minutes. The contents of the flask were transferred to 50 mL tubes after digestion, followed by centrifugation at 600 g for 5 minutes at room temperature. The cell pellet was resuspended in 40 mL saline and then centrifuged again at 600 g for 5 minutes at room temperature. After being resuspended again in 5-mL saline, the cell suspension was filtered through a 100 μm filter into a 50-mL conical tube to which 2 mL of saline was added to rinse the remaining cells through the filter. The flow-through was pipetted into a new 50-mL conical tube through a 40-μm filter. The tubes were centrifuged for the third time at 600 g for 5 minutes at room temperature. The cells were resuspended in saline. An aliquot of cell suspension was then removed for cell culture in Dulbecco's modified Eagle's medium (DMEM)-low glucose medium containing 10% FBS for 14 days. Approximately $2.0\text{-}3.0 \times 10^6$ ADMSCs were collected from each rat.

Exosomes preparation for SS treatment

The preparation, isolation and dosage of AD-MSC-derived exosomes have been descried in detail in our previous report [26]. Briefly, the exosomes were isolated from the culture medium of ADMSCs and pooled for protein separation and characterization, as well as western blot analysis. The proteins in Dulbecco's modified Eagle medium (DMEM) (Gibco) supplemented with 10% serum before and after cell culture were separated by sodium dodecyl sulfate-polyacrylamide gel electrophoresis (SDS-PAGE). The exosomes in DMEM were purified and the proteins in different exosome fractions (1 μg, 2 μg, 10 μg, and 50 μg) were also separated by SDS-PAGE. The gel was stained with Coomassie blue for analysis. The following primary antibodies were used: mouse monoclonal anti-CD63 (Santa Cruz Biotechnology), rabbit polyclonal anti-tumor susceptibility gene-101 (TSG101) (Abcam) and anti-β-catenin (Abcam).

Animal grouping, therapeutic strategy, blood sampling and time intervals of euthanized animals for individual study

The adult male SD rats (n = 72) were equally categorized into sham-operated control (SC, i.e., only opened the abdomen, then closed the muscle and skin layers), SS + 500 μ normal saline and SS + allogenic ADMSC-derived exosomes (AMSC^{EXO}) (i.e., 100 μg intravenous administration 3 h after CLP) groups. The exosome dosage administered was described in our previous report [24].

Blood samples were drawn at time intervals of 6, 16, 24 and 72 h for assessment of circulating levels of immune cells, cellular apoptosis and inflammatory biomarkers. Additionally, 6 animals in each group at these four time points were euthanized and brain tissues were harvested for individual study.

Isolation of splenic mononuclear cells for assessment of immune cells

Mononuclear cells in the spleen were isolated by homogenization of the spleen using a Ten-broeck tissue grinder followed by passage through a 0.4-mm-pore-size cell strainer to obtain a single cell suspension. These mononuclear cells were then suspended in RPMI and separated by Ficoll-paque Plus (GE Healthcare) for identification of immune cells.

Flow cytometric quantifications of inflammatory and apoptotic cells in circulation, and immune cells in circulation and spleen

The procedure and protocol of flow cytometric analysis which was performed to identify and characterize immune cells, apoptotic and inflammatory cell surface markers have been described in our previous reports [12, 24]. Briefly, peripheral blood mononuclear cells and splenocytes (1.0×10^6 cells for each population) were triple-stained with FITC-anti-CD3 (BioLegend), PE-anti-CD8a (BD Bioscience), and PE-Cy™5 anti-CD4 (BD bioscience). To identify CD4+CD25+Foxp3+ Tregs, peripheral blood mononuclear cells and splenocytes were triple-stained with Alexa Fluor 488-anti-CD25 (BioLegend), PE-anti-Foxp3 (BioLegend), and PE-Cy5 anti-CD4 (BD Bioscience) using the Foxp3 Fix/Perm buffer set according to the manufacturer's protocol. The numbers of CD3+/CD4+ helper T cells, CD3+/CD8+ cytotoxic T cells, and CD4+CD25+Foxp3+ Tregs were analyzed using flow cytometry (FC500, Beckman Coulter).

The percentages of viable and apoptotic cells were determined by flow cytometry using double staining of annexin V and propidium iodide

(PI). This is a simple and popular method for the identification of apoptotic cells (i.e., early [annexin V+/PI-] and late [annexin V+/PI+] phases of apoptosis).

Additionally, the numbers of inflammatory cells in circulation [i.e., CD11b/c, LyG6] were assessed using the flow cytometric method.

Analysis of circulating and cerebrospinal fluid (CSF) levels of inflammatory cytokines

Blood samples and CSF were drawn from rats in each group (n = 6/each time interval) at time points of 6, 24 and 72 h after SS induction and stored at -80°C until analyses of tumor necrosis factor (TNF)-α and interleukin (IL)-6 were performed in batches at the end of the experiment. Serum TNF-α and IL-6 concentrations were assessed in duplicate with a commercially available ELISA kit (R&D Systems, Minneapolis, MN, USA). Intra-individual variabilities in TNF-α and IL-6 levels were assessed in each group with the mean intra-assay coefficient of variance < 1.8%.

Immunohistochemical (IHC) and immunofluorescent (IF) staining

The procedure and protocol for IHC and IF staining have previously been reported in detail [12, 31, 32]. For IHC and IF staining, rehydrated paraffin sections were first treated with 3% H_2O_2 for 30 minutes and incubated with Immuno-Block reagent (BioSB, Santa Barbara, CA, USA) for 30 minutes at room temperature. Sections were then incubated with primary antibodies specifically against CD14 (1:200, Proteintech), F4/80 (1:100, Santa Cruz), glial fibrillary acidic protein (GFAP) (1:500, Dako) and MMP-9 (1:200, Themo Fisher Scientific) while sections incubated with irrelevant antibodies served as controls. Three kidney sections from each rat were analyzed. For quantification, three randomly selected HPFs (200× for IHC; 400× for IF) were analyzed in each section. The mean number of positively-stained cells per HPF for each animal was then determined by summation of all numbers divided by 9.

Western blot analysis

The procedure and protocol for Western blot analysis have been described in our previous reports [12, 31, 32]. Briefly, equal amounts (50

μg) of protein extract were loaded and separated by SDS-PAGE using acrylamide gradients. After electrophoresis, the separated proteins were transferred electrophoretically to a polyvinylidene difluoride (PVDF) membrane (Amersham Biosciences, Amersham, UK). Nonspecific sites were blocked by incubation of the membrane in blocking buffer [5% nonfat dry milk in T-TBS (TBS containing 0.05% Tween 20)] overnight. The membranes were incubated with the indicated primary antibodies [caspase 3 (1:1000, Cell Signaling, Danvers, MA, USA), Poly (ADP-ribose) polymerase (PARP) (1:1000, Cell Signaling, Danvers, MA, USA), high mobility group box protein 1 (HMGB1) (1:1000, Cell Signaling, Danvers, MA, USA), toll-like receptor 2 (TLR-2) (1:1000, Abcam, Cambridge, MA, USA), TLR-4 (1:1000, Novus Biologicals, Littleton, MA, USA), myeloid differentiation primary response 88 (MyD88) (1:1000, Abcam, Cambridge, MA, USA), tumor necrosis factor (TNF)-α (1:1000, Cell Signaling, Danvers, MA, USA), nuclear factor (NF)-κB (1:600, Abcam, Cambridge, MA, USA), NADPH oxidase (NOX)-1 (1:1500, Sigma, St. Louis, MO, USA), NOX-2 (1:750, Sigma, St. Louis, Mo, USA), interleukin (IL)-1ß (1:1000, Cell Signaling, Danvers, MA, USA), matrix metalloproteinase (MMP)-9 (1:1000, Abcam, Cambridge, MA, USA) and actin (1: 10000, Chemicon, Billerica, MA, USA)] for 1 hour at room temperature. Horseradish peroxidase-conjugated anti-rabbit immunoglobulin IgG (1:2000, Cell Signaling, Danvers, MA, USA) was used as a secondary antibody for one-hour incubation at room temperature. The washing procedure was repeated eight times within one hour. Immunoreactive bands were visualized by enhanced chemiluminescence (ECL; Amersham Biosciences, Amersham, UK) and exposed to Biomax L film (Kodak, Rochester, NY, USA). For quantification, ECL signals were digitized using Labwork software (UVP, Waltham, MA, USA). The full gel images of western blot were available in the Figure S1.

Assessment of oxidative stress

The procedure and protocol for assessing the protein expression of oxidative stress have been detailed in our previous reports [12, 31, 32]. The Oxyblot Oxidized Protein Detection Kit was purchased from Chemicon, Billerica, MA, USA (S7150). DNPH derivatization was carried out on 6 μg of protein for 15 minutes according to the manufacturer's instructions. One-dimen-

sional electrophoresis was carried out on 12% SDS/polyacrylamide gel after DNPH derivatization. Proteins were transferred to nitrocellulose membranes which were then incubated in the primary antibody solution (anti-DNP 1:150) for 2 hours, followed by incubation in secondary antibody solution (1:300) for 1 hour at room temperature. The washing procedure was repeated eight times within 40 minutes.

Immunoreactive bands were visualized by enhanced chemiluminescence (ECL; Amersham Biosciences, Amersham, UK) which was then exposed to Biomax L film (Kodak, Rochester, NY, USA). For quantification, ECL signals were digitized using Labwork software (UVP, Waltham, MA, USA). For Oxyblot protein analysis, a standard control was loaded on each gel.

Statistical analysis

Quantitative data are expressed as means ± SD. Statistical analysis was adequately performed by ANOVA followed by Bonferroni multiple-comparison post hoc test. Statistical analysis was performed using SPSS statistical software for Windows version 22 (SPSS for Windows, version 22; SPSS, IL, USA). A value of $P < 0.05$ was considered as statistically significant.

Results

*Circulating levels of inflammatory and apoptotic cells at time points of 6, 16, 24 and 72 h after SS induction (**Figure 1**)*

The circulating numbers of Ly6G+ and CD11[b/c]+ cells, two indicators of inflammation, were significantly higher in group 2 (SS) than in group 1 (SC) and group 3 (SS + AMSC[EXO]), and significantly higher in group 3 than in group 1 at time intervals of 6, 16, 24 and 72 h. Additionally, the circulating levels of early (i.e., annexin V+/PI-] and late [i.e., annexin V+/PI+] cellular apoptosis also exhibited an identical pattern of inflammatory cells at time intervals of 6, 16, 24 and 72 h.

*Serial changes of immune cells in circulation and spleen (**Figures 2** and **3**)*

The circulating and splenic levels of CD3+/CD4+ cells and CD3+/CD8+ cells, two indices of immune reaction, were significantly incre-

ased in group 2 than in groups 1 and 3, and significantly increased in group 3 than in group 1 at time points of 6, 16, 24, and 72 h (**Figure 2**). On the other hand, the circulating and splenic levels of T-reg+ cells, an indicator of immunomodulation, were progressively increased from groups 1 to 3, highlighting an intrinsic response to inflammatory reaction in SS than the corresponding MSC[EXO]-enhanced treatment for purpose of attenuating the overwhelming immune response in SS (**Figure 3**).

*Measurement of circulating and CSF levels of inflammatory cytokines by ELISA at time intervals of 6, 24, and 72 h after SS induction (**Figure 4**)*

The circulating and CSF levels of TNF-α and IL-6, two indicators of acute inflammatory cytokines, were significantly increased in group 2 than in groups 1 and 3, and significantly increased in group 3 than in group 1 at time intervals of 6, 24 and 72 h.

*Inflammatory cell infiltration in brain tissues by time intervals of 6 and 72 h after SS induction (**Figures 5** and **6**)*

The cellular expressions of F4/80 and CD14, two indicators of inflammation, at time points of 6 and 72 h after SS induction, were significantly higher in group 2 than in groups 1 and 3, and significantly higher in group 3 than in group 1 (**Figure 5**). Additionally, cellular expressions of MMP-9 and GFAP, another two indicators of inflammation, exhibited an identical pattern of CD14 among the three groups at these two time points (**Figure 6**).

*Cellular expressions of brain-damaged biomarkers at time intervals of 6 and 72 h after SS induction (**Figure 7**)*

The cellular expressions of AQP4 (i.e., brain edema index) and γ-H2AX (DNA-damaged indicator) were significantly increased in group 2 as compared to those of groups 1 and 3 and significantly higher in group 3 than in group 1.

*Protein levels of apoptotic and brain damaged released inflammatory biomarkers at time intervals of 6 and 72 h after SS induction (**Figure 8**)*

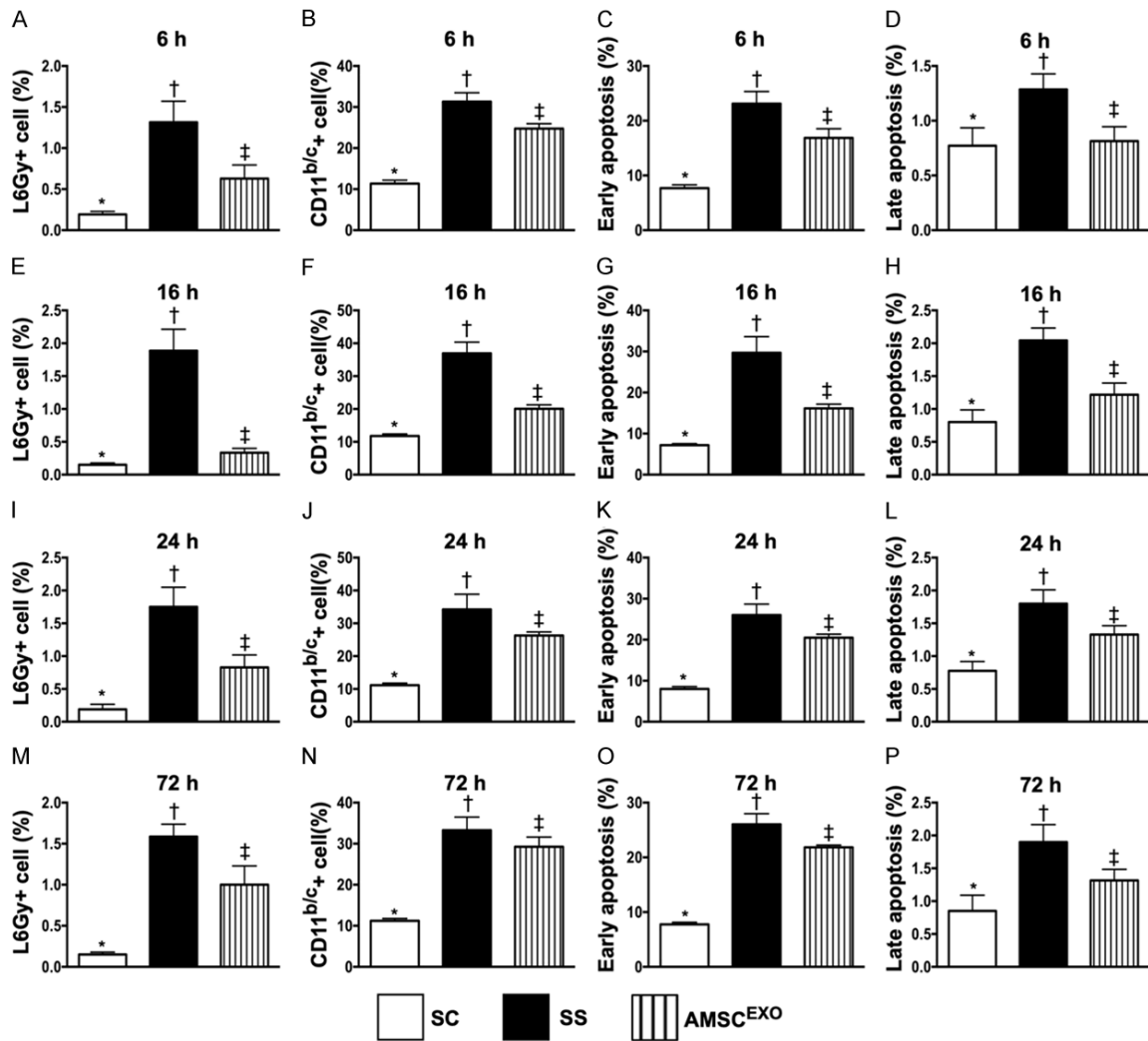The protein expressions of cleaved caspase 3 and cleaved PARP, two indicators of apoptotic

Figure 1. Circulating levels of inflammatory and apoptotic cells at time points of 6, 16, 24 and 72 h after SS induction. (A-D) Circulating numbers of Ly6G+ cells (A), CD11$^{b/c}$+ cells (B), early apoptotic cells (C) and late apoptotic cells (D) at 6 h, *vs. other groups with different symbols (†, ‡), P < 0.001, respectively. (E-H) Circulating numbers of Ly6G+ cells (E), CD11$^{b/c}$+ cells (F), early apoptotic cells (G) and late apoptotic cells (H) at 16 h, *vs. other groups with different symbols (†, ‡), P < 0.0001, respectively. (I-L) Circulating numbers of Ly6G+ cells (I), CD11$^{b/c}$+ cells (J), early apoptotic cells (K) and late apoptotic cells (L) at 24 h, *vs. other groups with different symbols (†, ‡), P < 0.0001, respectively. (M-P) Circulating numbers of Ly6G+ cells (M), CD11$^{b/c}$+ cells (N), early apoptotic cells (O) and late apoptotic cells (P) at 72 h, *vs. other groups with different symbols (†, ‡), P < 0.001, respectively. All statistical analyses were performed by one-way ANOVA, followed by Bonferroni multiple comparison post hoc test (n = 6 for each group). Symbols (*, †, ‡) indicate significance (at 0.05 level). SC = sham-operated control; SS = sepsis syndrome; AMSC^{EXO} = allogenic adipose-derived mesenchymal stem cells-derived exosomes.

biomarkers, were significantly higher in group 2 than in groups 1 and 3, and significantly higher in group 3 than in group 1 at time intervals of 6 and 72 h after SS induction.

Additionally, protein expression of high mobility group box protein 1 (HMGB1), a component of damage-associated molecular patterns (DAM-Ps), displayed an identical pattern of apoptosis

among the three groups at these two-time intervals.

*The protein expressions of inflammatory biomarkers at time intervals of 6 and 72 h after SS induction (**Figures 9** and **10**)*

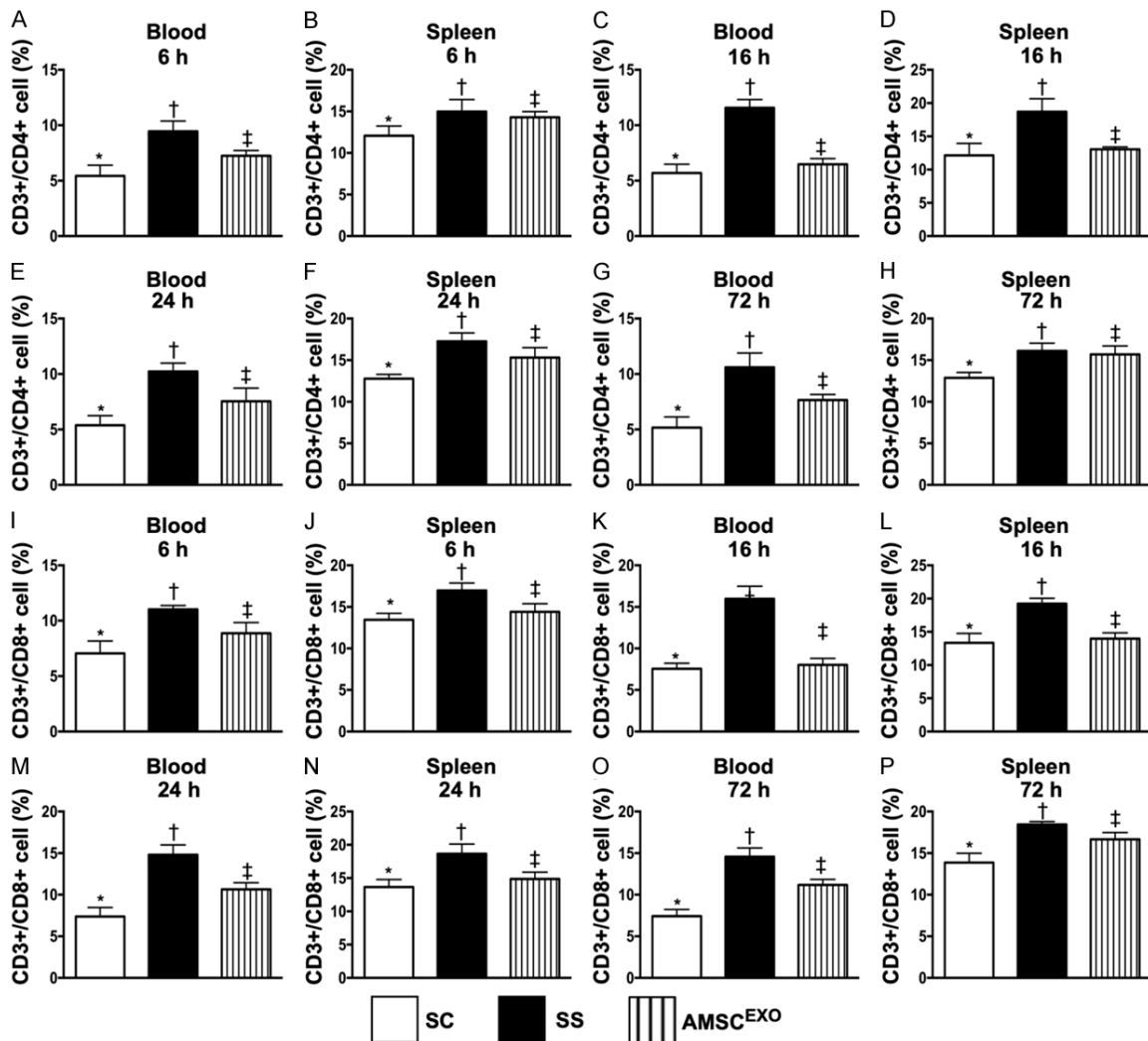The protein expressions of TLR-2, TLR-4, and MyD88, three indices of inflammation, were

Figure 2. Circulatory and splenic levels of immune cells at time intervals of 6, 16, 24 and 72 h after SS induction. (A, B) Number of CD3+/CD4+ cells in circulation (A) and spleen (B) at 6 h, *vs. other groups with different symbols (†, ‡), P < 0.001. (C, D) Number of CD3+/CD4+ cells in circulation (C) and spleen (D) at 16 h, *vs. other groups with different symbols (†, ‡), P < 0.0001. (E, F) Number of CD3+/CD4+ cells in circulation (E) and spleen (F) at 24 h, *vs. other groups with different symbols (†, ‡), P < 0.0001. (G, H) Number of CD3+/CD4+ cells in circulation (G) and spleen (H) at 72 h, *vs. other groups with different symbols (†, ‡), P < 0.001. (I, J) Number of CD3+/CD8+ cells in circulation (I) and spleen (J) at 6 h, *vs. other groups with different symbols (†, ‡), P < 0.001. (K, L) Number of CD3+/CD8+ cells in circulation (K) and spleen (L) at 16 h, *vs. other groups with different symbols (†, ‡), P < 0.0001. (M, N) Number of CD3+/CD8+ cells in circulation (M) and spleen (N) at 24 h, *vs. other groups with different symbols (†, ‡), P < 0.001. (O, P) Number of CD3+/CD8+ cells in circulation (O) and spleen (P) at 72 h, *vs. other groups with different symbols (†, ‡), P < 0.001. All statistical analyses were performed by one-way ANOVA, followed by Bonferroni multiple comparison post hoc test (n = 6 for each group). Symbols (*, †, ‡) indicate significance (at 0.05 level). SC = sham-operated control; SS = sepsis syndrome; AMSC^EXO = allogenic adipose-derived mesenchymal stem cells-derived exosomes.

significantly higher in group 2 than in groups 1 and 3, and significantly higher in group 3 than in group 1 at time intervals of 6 and 72 h after SS induction (**Figure 9**). Furthermore, the protein expressions of IL-1β, MMP-9, TNF-α and NF-κB, another four indicators of inflammatory biomarkers, displayed an identical pattern of MyD88 among the three groups at these two-time intervals (**Figure 10**).

*The protein expressions of oxidative-stress biomarkers at time intervals of 6 and 72 h after SS induction (**Figure 11**)*

The protein expressions of NOX-1, NOX-2 and oxidized protein, three indicators of oxidative stress, were significantly increased in group 2 than in groups 1 and 3, and significantly increased in group 3 than in group 1 at time intervals of 6 and 72 h after SS induction.
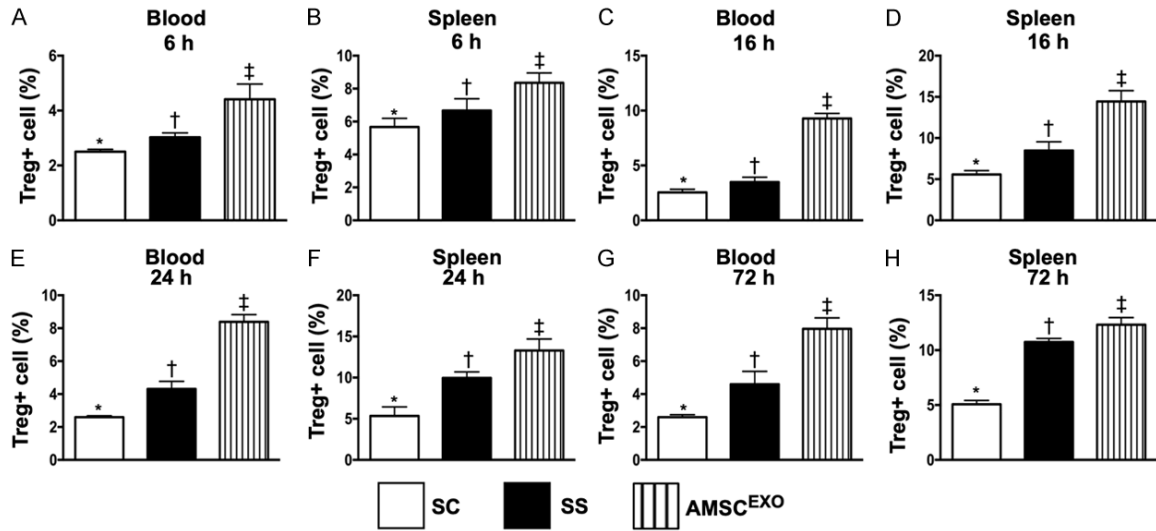
Figure 3. Circulatory and splenic levels of T-reg+ cells at time intervals of 6, 16, 24 and 72 h after SS induction. (A, B) Number of T-reg+ cells in circulation (A) and spleen (B) ay 6 h, *vs. other groups with different symbols (†, ‡), P < 0.001. (C, D) Number of T-reg+ cells in circulation (C) and spleen (D) ay 16 h, *vs. other groups with different symbols (†, ‡), P < 0.0001. (E, F) Number of T-reg+ cells in circulation (E) and spleen (F) ay 24 h, *vs. other groups with different symbols (†, ‡), P < 0.0001. (G, H) Number of T-reg+ cells in circulation (G) and spleen (H) ay 72 h, *vs. other groups with different symbols (†, ‡), P < 0.0001. All statistical analyses were performed by one-way ANOVA, followed by Bonferroni multiple comparison post hoc test (n = 6 for each group). Symbols (*, †, ‡) indicate significance (at 0.05 level). SC = sham-operated control; SS = sepsis syndrome; AMSC^{EXO} = allogenic adipose-derived mesenchymal stem cells-derived exosomes.
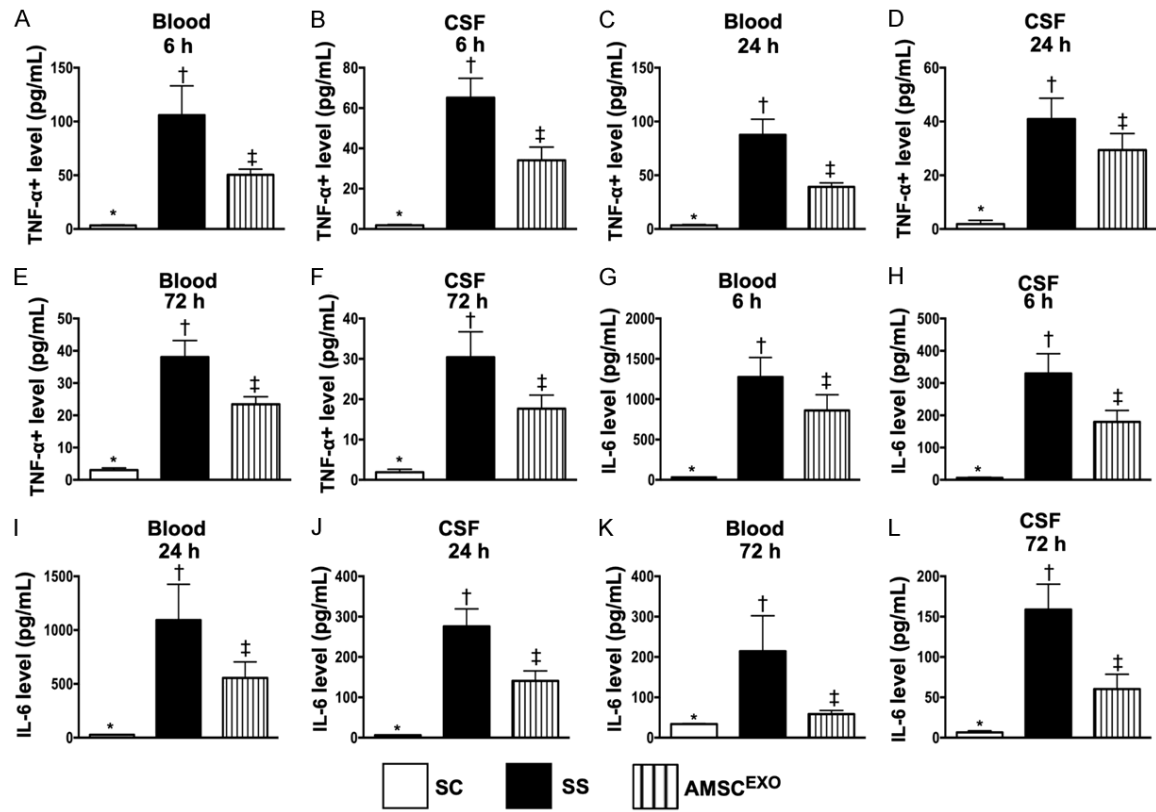

Figure 4. Measurement of circulating and CSF levels of inflammatory cytokines by ELISA at time intervals of 6, 24, and 72 h after SS induction. (A, B) Level of tumor necrosis factor (TNF)-α in circulation (A) and Cerebrospinal fluid

(CSF) (B) at 6 h, *vs. other groups with different symbols (†, ‡), P < 0.0001. (C, D) Level of TNF-α in circulation (C) and CSF (D) at 24 h, *vs. other groups with different symbols (†, ‡), P < 0.0001. (E, F) Level of TNF-α in circulation (E) and CSF (F) at 72 h, *vs. other groups with different symbols (†, ‡), P < 0.0001. (G, H) Level of interleukin (IL)-6 in circulation (G) and CSF (H) at 6 h, *vs. other groups with different symbols (†, ‡), P < 0.0001. (I, J) Level of IL-6 in circulation (I) and CSF (J) at 24 h, *vs. other groups with different symbols (†, ‡), P < 0.0001. (K, L) level of IL-6 in circulation (K) and CSF (L) at 72 h, *vs. other groups with different symbols (†, ‡), P < 0.0001. All statistical analyses were performed by one-way ANOVA, followed by Bonferroni multiple comparison post hoc test (n = 6 for each group). Symbols (*, †, ‡) indicate significance (at 0.05 level). SC = sham-operated control; SS = sepsis syndrome; AMSC^{EXO} = allogenic adipose-derived mesenchymal stem cells-derived exosomes.
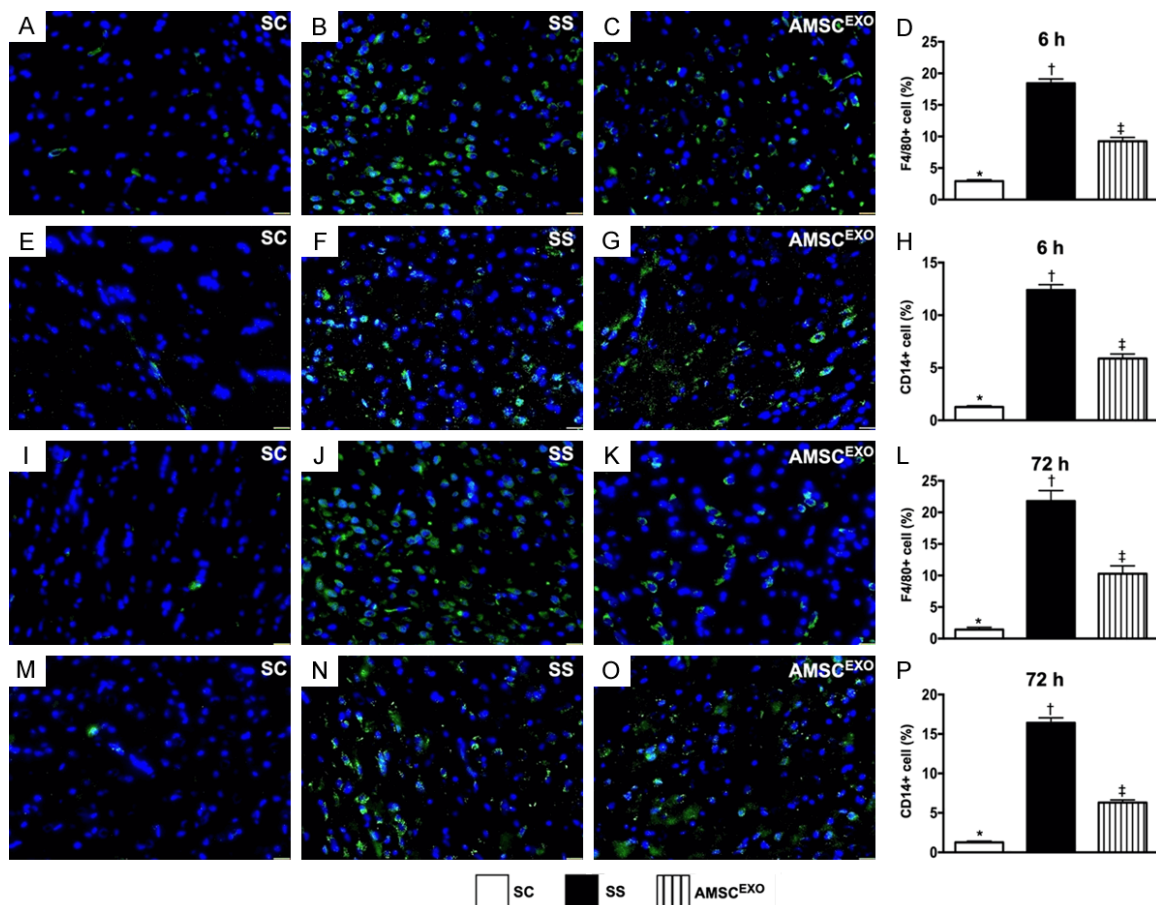

Figure 5. Inflammatory cell infiltration in brain tissues by time intervals of 6 and 72 h after SS induction. A-C. Illustrating the immunofluorescent (IF) microscopic finding (400×) for identification of cellular expression of F4/80 at 6 h (green color). D. Analytical result of number of F4/80+ cells, *vs. other groups with different symbols (†, ‡), P < 0.0001. E-G. Illustrating the IF microscopic finding (400×) for identification of cellular expression of CD14 at 6 h (green color). H. Analytical result of number of CD14+ cells, *vs. other groups with different symbols (†, ‡), P < 0.0001. I-K Illustrating the IF microscopic finding (400×) for identification of cellular expression of F4/80 at 72 h (green color). L. Analytical result of number of F4/80+ cells, *vs. other groups with different symbols (†, ‡), P < 0.0001. M-O. Illustrating the IF microscopic finding (400×) for identification of cellular expression of CD14 at 72 h (green color). P. Analytical result of number of CD14+ cells, *vs. other groups with different symbols (†, ‡), P < 0.0001. Blue color indicted the nuclei stained by DAPI. Scale bars in lower right corner represent 20 μm. All statistical analyses were performed by one-way ANOVA, followed by Bonferroni multiple comparison post hoc test (n = 6 for each group). Symbols (*, †, ‡) indicate significance (at 0.05 level). SC = sham-operated control; SS = sepsis syndrome; AMSC^{EXO} = allogenic adipose-derived mesenchymal stem cells-derived exosomes.

Discussion

This study which investigated the therapeutic impact of ADMSC-derived exosomes on pro-

tecting the brain from SS-induced brain damage yielded several striking implications. Frist, the results of this current study showed that original source of abdominal sepsis elicited not
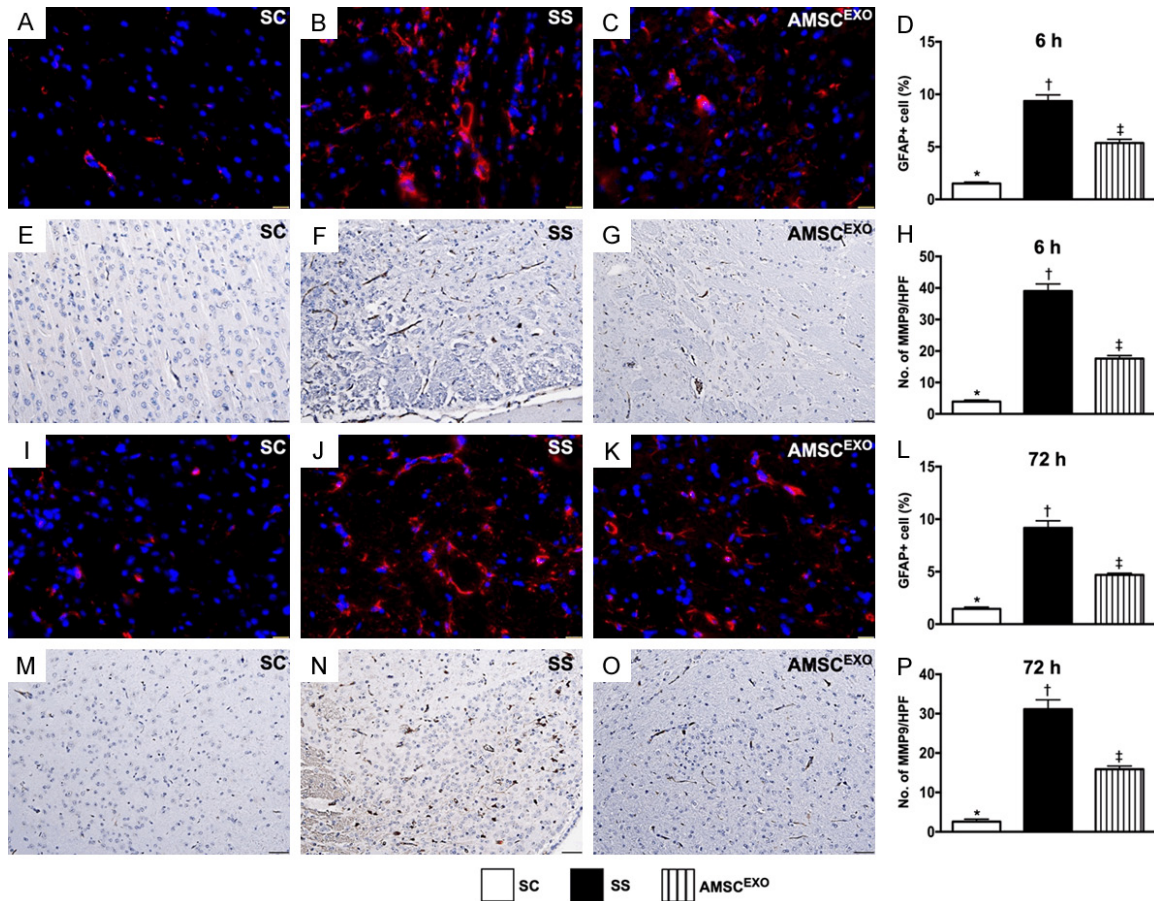
Figure 6. Inflammatory cell biomarkers in brain tissues by time intervals of 6 and 72 h after SS induction. A-C. Illustrating the immunofluorescent (IF) microscopic finding (400×) for identification of cellular expression of glial fibrillary acidic protein (GFAP) at 6 h (red color). D. Analytical result of number of GFAP+ cells, *vs. other groups with different symbols (†, ‡), P < 0.0001. Scale bars in lower right corner represent 20 μm. E-G. Illustrating the immunohistochemical (IHC) stain for identifying the cellular expression of matrix metalloproteinase (MMP)-9 (gray color). H. Analytical result of number of MMP-9+ cells, *vs. other groups with different symbols (†, ‡), P < 0.0001. Scale bars in lower right corner represent 50 μm. I-K. Illustrating the IF microscopic finding (400×) for identification of cellular expression of glial fibrillary acidic protein (GFAP) at 72 h (red color). L. Analytical result of number of GFAP+ cells, *vs. other groups with different symbols (†, ‡), P < 0.0001. Scale bars in lower right corner represent 20 μm. M-O. Illustrating the IHC stain for identifying the cellular expression of MMP-9 (gray color). P. Analytical result of number of MMP-9+ cells, *vs. other groups with different symbols (†, ‡), P < 0.0001. HPF = high-power field. Blue color indicated nuclei stained by DAPI. Scale bars in lower right corner represent 50 μm. All statistical analyses were performed by one-way ANOVA, followed by Bonferroni multiple comparison post hoc test (n = 6 for each group). Symbols (*, †, ‡) indicate significance (at 0.05 level). SC = sham-operated control; SS = sepsis syndrome; AMSC[EXO] = allogenic adipose-derived mesenchymal stem cells-derived exosomes.

only circulatory inflammatory reaction but also brain organ inflammatory response (i.e., a "sepsis victim" as likely as other organs), highlighting that SS affected systemically and involved multiple innocent organs. Second, the time points of measuring inflammatory biomarkers demonstrated that the vigorous immune-inflammatory reactions emerged at a peak level as early as a few hours (i.e., ≤ 6 h) after SS induction that were not only in circulatory but also extended to brain organ and CSF. Third,

prompt administration of ADMSC-derived exosomes effectively suppressed the systemic immune-inflammatory responses and protected the brain organ from SS-induced damage.

Whatever the original source of infection is, vast previous studies have shown that sepsis can spread into circulation causing SS which ultimately leads to multiple organ failure and unacceptably high mortality [1-5, 9, 10]. A principal finding in the present study was that the
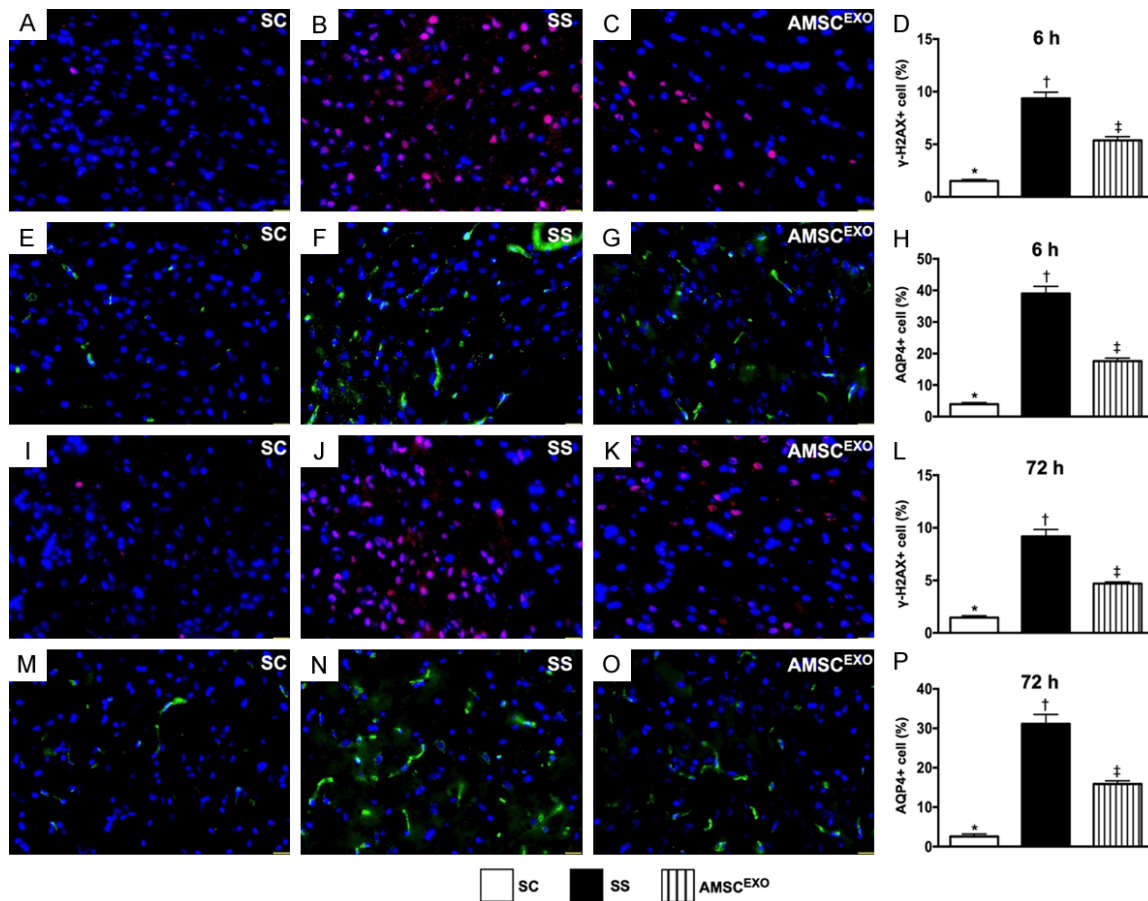
Figure 7. Cellular expressions of brain-damaged biomarkers at time intervals of 6 and 72 h after SS induction. A-C. Illustrating the immunofluorescent (IF) microscopic finding (400×) for identification of cellular expression of γ-H2AX at 6 h (pink color). D. Analytical result of number of γ-H2AX+ cells, *vs. other groups with different symbols (†, ‡), P < 0.0001. E-G. Illustrating the IF microscopic finding (400×) for identification of cellular expression of Aquaporin-4 (AQP4) at 6 h (green color). H. Analytical result of number of AQP4+ cells, *vs. other groups with different symbols (†, ‡), P < 0.0001. I-K. Illustrating the IF microscopic finding (400×) for identification of cellular expression of γ-H2AX at 72 h (pink color). L. Analytical result of number of γ-H2AX+ cells, *vs. other groups with different symbols (†, ‡), P < 0.0001. M-O. Illustrating the IF microscopic finding (400×) for identification of cellular expression of AQP4 at 72 h (green color). P. Analytical result of number of AQP4+ cells, *vs. other groups with different symbols (†, ‡), P < 0.0001. Blue color indicated nuclei stained by DAPI. Scale bars in lower right corner represent 20 μm. All statistical analyses were performed by one-way ANOVA, followed by Bonferroni multiple comparison post hoc test (n = 6 for each group). Symbols (*, †, ‡) indicate significance (at 0.05 level). SC = sham-operated control; SS = sepsis syndrome; AMSC^EXO = allogenic adipose-derived mesenchymal stem cells-derived exosomes.

immune-inflammatory reactions were identified not only in the circulation, but also in spleen as well as in the brain tissue and CSF, indicating that an abdominal origin of SS could disseminate throughout the human body. Our results using an experimental study support the findings from previous clinical trials and observational studies [1-5, 9, 10].

Intriguingly, even though the sepsis-associated encephalopathy and the incidence of SS-associated metabolic disturbance and CNS com-

plication as well as its unfavorable prognostic outcome have been earnestly clarified, yet regrettably the underlying mechanisms remain a heatedly debated topic [14-18]. An essential finding in the present study was that not only the cytokine level but also molecular-cellular and protein levels of inflammatory biomarkers were identified to markedly increase in CNS (i.e., expressed in brain tissues and CSF) in SS animals. Our findings, could, at least in part, explain the phenomena of CNS complications after sepsis that have been revealed by previ-
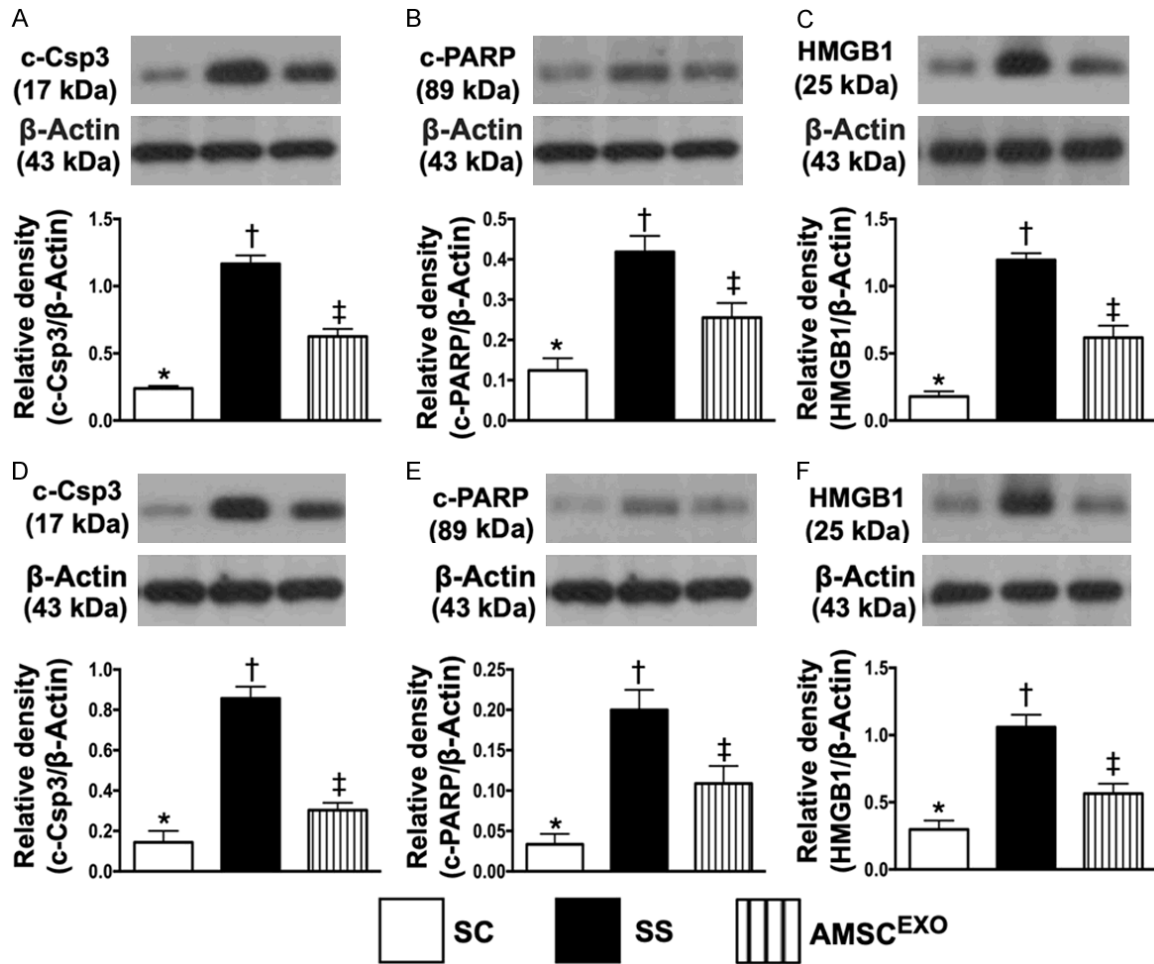
Figure 8. Protein levels of apoptotic and brain-damaged released biomarkers at time intervals of 6 and 72 h after SS induction. A. Protein expression of cleaved caspase 3 (c-Csp-3) at 6 h, *vs. other groups with different symbols (†, ‡), P < 0.0001. B. Protein expression of cleaved Poly (ADP-ribose) polymerase (c-PARP) at 6 h, *vs. other groups with different symbols (†, ‡), P < 0.0001. C. Protein expression of high mobility group box protein 1 (HMGB1) at 6 h, *vs. other groups with different symbols (†, ‡), P < 0.0001. D. Protein expression of c-Csp-3 at 72 h, *vs. other groups with different symbols (†, ‡), P < 0.0001. E. Protein expression of c-PARP at 72 h, *vs. other groups with different symbols (†, ‡), P < 0.0001. F. Protein expression of HMGB1 at 72 h, *vs. other groups with different symbols (†, ‡), P < 0.0001. All statistical analyses were performed by one-way ANOVA, followed by Bonferroni multiple comparison post hoc test (n = 6 for each group). Symbols (*, †, ‡) indicate significance (at 0.05 level). SC = sham-operated control; SS = sepsis syndrome; AMSC^{EXO} = allogenic adipose-derived mesenchymal stem cells-derived exosomes.

ous clinical findings [14-18]. Interestingly, some studies have proposed that systemic inflammation appears to play a crucial role in both altering the blood-brain barrier (BBB) permeability and amplifying the inflammatory response [15]. This may partially explain why the inflammatory mediators could penetrate the brain organ (i.e., BBB permeability increased) and elicit encephalopathy in setting of SS.

Our recent study has demonstrated that DAMPs inflammatory axis was markedly upregulated and participated in brain damage in brain-death animals [33]. The most important finding in the present study was that the levels of a DAMP component (i.e., HMGB1) and downstream inflammatory biomarkers, i.e., TLR-2, TLR-4, MYD88, IL-1β, TNF-α, NF-κB and MMP-9, were substantially higher in brain tissue from SS animals than the SC. In this way, our findings, in addition to being consistent with the results of our recent study [33], could powerfully explain why the brain is frequently as an innocent victim seriously damaged by SS, highlighting that not only the brain is an organ failing in sepsis but also sepsis overwhelmingly
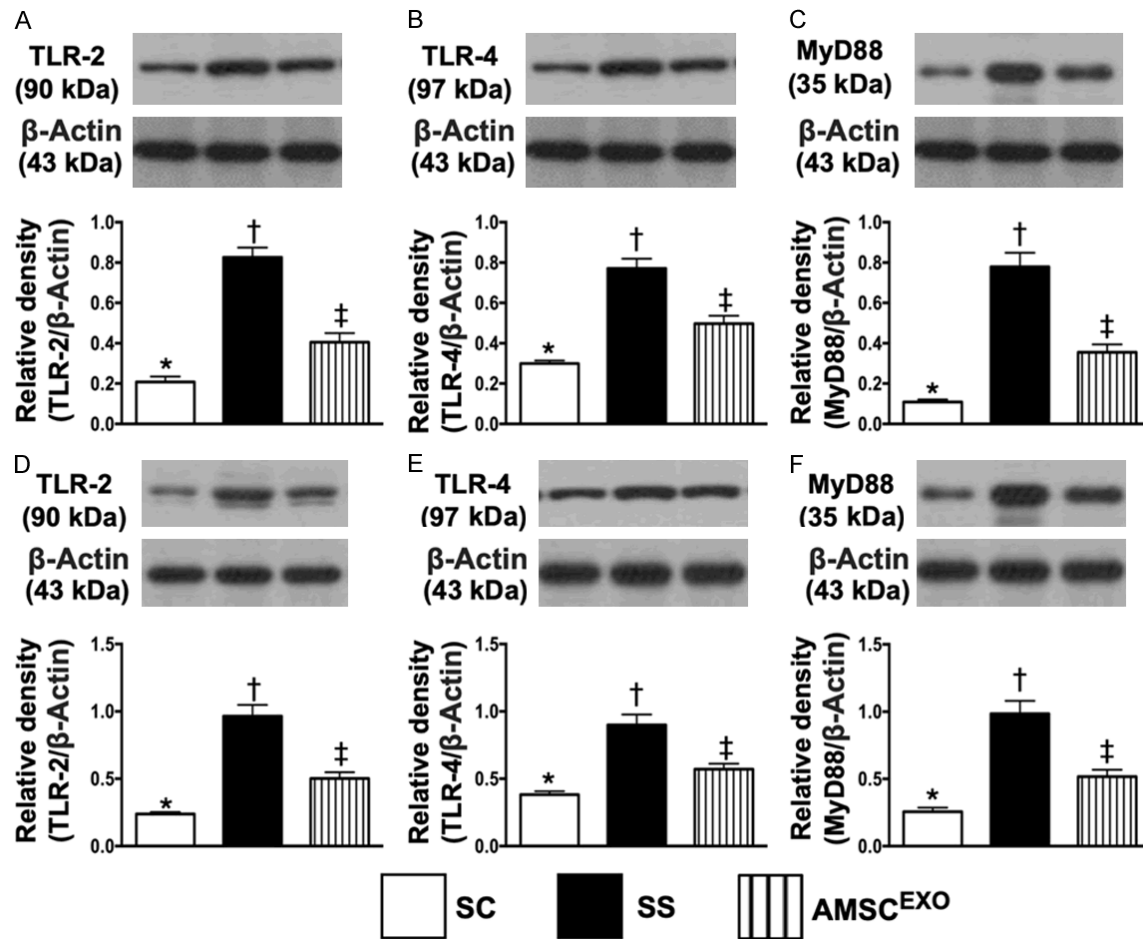
Figure 9. Protein levels of upstream inflammatory biomarkers at time intervals of 6 and 72 h after SS induction. A. Protein expression of toll-like receptor (TLR)-2 at 6 h, *vs. other groups with different symbols (†, ‡), P < 0.0001. B. Protein expression of TLR-4 at 6 h, *vs. other groups with different symbols (†, ‡), P < 0.0001. C. Protein expression of myeloid differentiation primary response 88 (MyD88) at 6 h, *vs. other groups with different symbols (†, ‡), P < 0.0001. D. Protein expression of TLR-2 at 72 h, *vs. other groups with different symbols (†, ‡), P < 0.0001. E. Protein expression of TLR-4 at 72 h, *vs. other groups with different symbols (†, ‡), P < 0.0001. F. Protein expression of MyD88 at 72 h, *vs. other groups with different symbols (†, ‡), P < 0.0001. All statistical analyses were performed by one-way ANOVA, followed by Bonferroni multiple comparison post hoc test (n = 6 for each group). Symbols (*, †, ‡) indicate significance (at 0.05 level). SC = sham-operated control; SS = sepsis syndrome; AMSC^EXO = allogenic adipose-derived mesenchymal stem cells-derived exosomes.

influences all inflammatory processes on a variety of pathophysiologic levels, thus contributes to the initiation and propagation of septic processes [17]. Of particular importance was that these molecular-cellular perturbations in circulatory and splenic levels and in brain tissue as well as in CSF were remarkably suppressed by ADMSC-derived exosomes. Intriguingly, ours [24, 26, 29, 30] and other studies [15, 23, 25, 27, 28] have previously shown that MSC-derived exosomes protected the organs from ischemia/ischemia-reperfusion injury or from sepsis-induced damage mainly through immunomodulation and suppression of the inflammatory reaction and oxidative stress. In this

way, the results of the current study, in addition to being consistent with the findings of the previous studies [15, 23-30], highlight that these preclinical findings convey a significant clinical information that ADMSC-derived exosomes may have a potential therapeutic impact on the setting of SS complicated with CNS involvement, especially in patients who are refractory to conventional treatment.

Study limitations

This study has limitations. First, the neurological function was not examined in the present
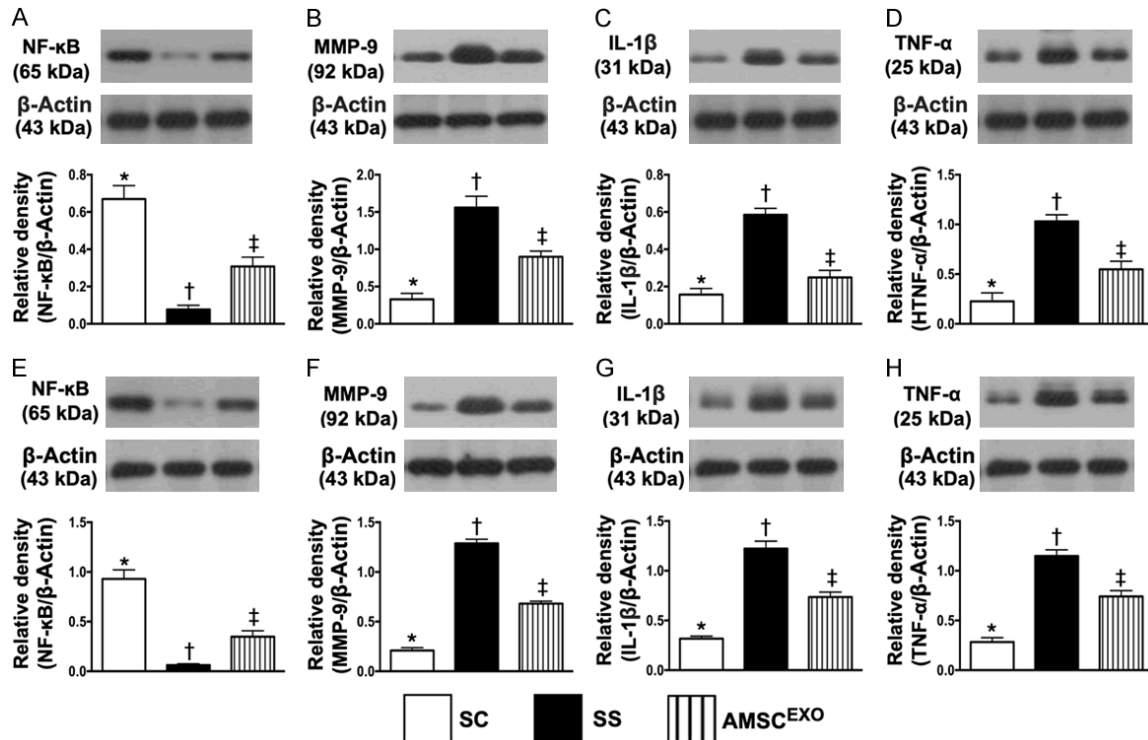
Figure 10. The protein expressions of downstream inflammatory biomarkers at time intervals of 6 and 72 h after SS induction. A. Protein expression of nuclear factor (NF)-κB at 6 h, *vs. other groups with different symbols (†, ‡), P < 0.0001. B. Protein expression of matrix metalloproteinase (MMP)-9 at 6 h, *vs. other groups with different symbols (†, ‡), P < 0.0001. C. Protein expression interleukin (IL)-1ß at 6 h, *vs. other groups with different symbols (†, ‡), P < 0.0001. D. Protein expression of tumor necrosis factor (TNF)-α at 6 h, *vs. other groups with different symbols (†, ‡), P < 0.0001. E. Protein expression of NF-κB at 72 h, *vs. other groups with different symbols (†, ‡), P < 0.0001. F. Protein expression of MMP-9 at 72 h, *vs. other groups with different symbols (†, ‡), P < 0.0001. G. Protein expression IL-1β at 72 h, *vs. other groups with different symbols (†, ‡), P < 0.0001. H. Protein expression of TNF-α at 72 h, *vs. other groups with different symbols (†, ‡), P < 0.0001. All statistical analyses were performed by one-way ANOVA, followed by Bonferroni multiple comparison post hoc test (n = 6 for each group). Symbols (*, †, ‡) indicate significance (at 0.05 level). SC = sham-operated control; SS = sepsis syndrome; AMSC^EXO = allogenic adipose-derived mesenchymal stem cells-derived exosomes.

study. Thus, we did not provide the information regarding the impairment of neurological function in setting of SS and the recovery of the neurological status after ADMSC-derived exosome therapy. Second, the study period was relatively short. As a consequence, the long-term outcome of ADMSC-derived exosome therapy on protecting the brain against SS injury remains to be clarified.

In conclusion, allogenic ADMSC-derived exosome therapy significantly protected the brain from SS-induced damage.

Disclosure of conflict of interest

None.

Address correspondence to: Hon-Kan Yip, Division of Cardiology, Department of Internal Medicine, Kaohsiung Chang Gung Memorial Hospital and Chang Gung University College of Medicine, Kaohsiung 83301, Taiwan. Tel: 886-7-7317123 Ext. 8300; Fax: 886-7-7322402; E-mail: han.gung@msa.hinet.net; Chia-Lo Chang, Division of Colorectal Surgery, Department of Surgery, Kaohsiung Chang Gung Memorial Hospital, 123 Dapi Road, Niaosung District, Kaohsiung 833-01, Taiwan. Tel: 886-7-7317123 Ext. 8300; Fax: 886-7-7322402; E-mail: 168leo168@gmail.com
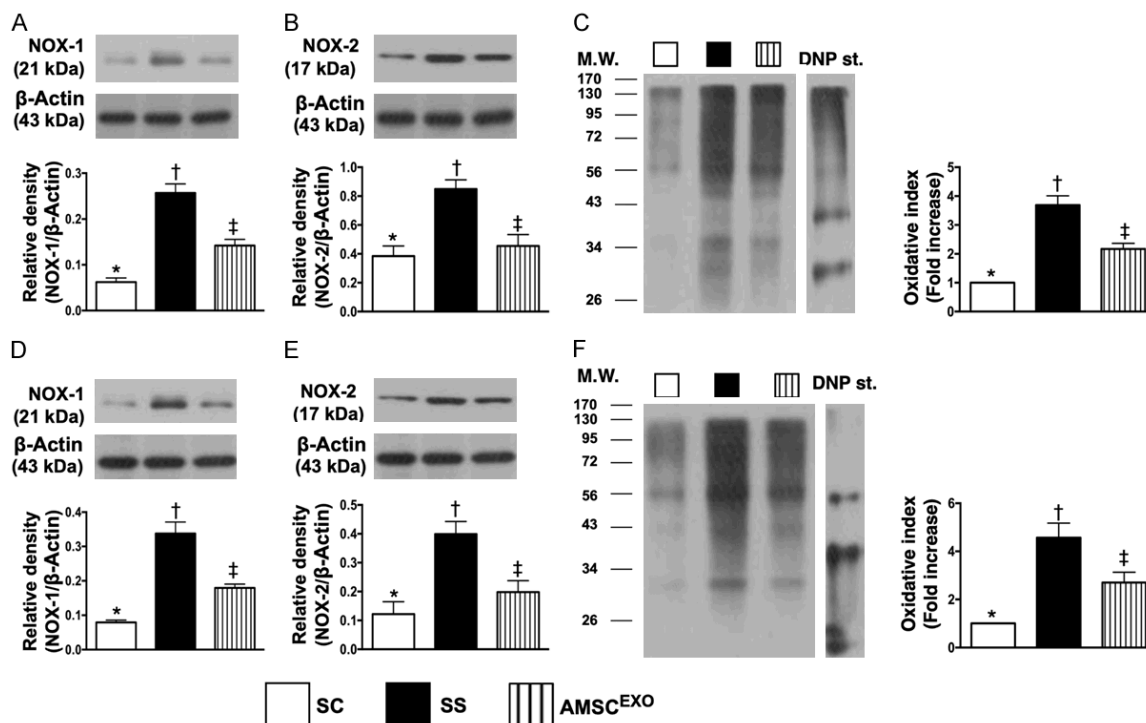
Figure 11. Protein expressions of oxidative-stress biomarkers at time intervals of 6 and 72 h after SS induction. A. Protein expression of NOX-1 at 6 h, *vs. other groups with different symbols (†, ‡), P < 0.0001. B. Protein expression of NOX-2 at 6 h, *vs. other groups with different symbols (†, ‡), P < 0.0001. C. Oxidized protein expression at 6 h, *vs. other groups with different symbols (†, ‡), P < 0.0001. (Note: left and right lanes shown on the upper panel represent protein molecular weight marker and control oxidized molecular protein standard, respectively). MW = molecular weight; DNP = 1-3 dinitrophenylhydrazone. D. Protein expression of NOX-1 at 72 h, *vs. other groups with different symbols (†, ‡), P < 0.0001. E. Protein expression of NOX-2 at 72 h, *vs. other groups with different symbols (†, ‡), P < 0.0001. F. Oxidized protein expression at 72 h, *vs. other groups with different symbols (†, ‡), P < 0.0001. All statistical analyses were performed by one-way ANOVA, followed by Bonferroni multiple comparison post hoc test (n = 6 for each group). Symbols (*, †, ‡) indicate significance (at 0.05 level). SC = sham-operated control; SS = sepsis syndrome; AMSC^EXO = allogenic adipose-derived mesenchymal stem cells-derived exosomes.

References

[1] Angus DC, Linde-Zwirble WT, Lidicker J, Clermont G, Carcillo J, Pinsky MR. Epidemiology of severe sepsis in the United States: analysis of incidence, outcome, and associated costs of care. Crit Care Med 2001; 29: 1303-1310.

[2] Brun-Buisson C, Meshaka P, Pinton P, Vallet B, Group ES. EPISEPSIS: a reappraisal of the epidemiology and outcome of severe sepsis in French intensive care units. Intensive Care Med 2004; 30: 580-588.

[3] Brun-Buisson C, Roudot-Thoraval F, Girou E, Grenier-Sennelier C, Durand-Zaleski I. The costs of septic syndromes in the intensive care unit and influence of hospital-acquired sepsis. Intensive Care Med 2003; 29: 1464-1471.

[4] Dellinger RP, Levy MM, Carlet JM, Bion J, Parker MM, Jaeschke R, Reinhart K, Angus DC, Brun-Buisson C, Beale R, Calandra T, Dhainaut JF, Gerlach H, Harvey M, Marini JJ, Marshall J, Ranieri M, Ramsay G, Sevransky J, Thompson BT, Townsend S, Vender JS, Zimmerman JL, Vincent JL. Surviving Sepsis Campaign: international guidelines for management of severe sepsis and septic shock: 2008. Intensive Care Med 2008; 34: 17-60.

[5] Dellinger RP, Levy MM, Rhodes A, Annane D, Gerlach H, Opal SM, Sevransky JE, Sprung CL, Douglas IS, Jaeschke R, Osborn TM, Nunnally ME, Townsend SR, Reinhart K, Kleinpell RM, Angus DC, Deutschman CS, Machado FR, Rubenfeld GD, Webb SA, Beale RJ, Vincent JL, Moreno R; Surviving Sepsis Campaign Guidelines Committee including The Pediatric Subgroup. Surviving sepsis campaign: international guidelines for management of severe sepsis and septic shock, 2012. Intensive Care Med 2013; 39: 165-228.

[6] Seymour CW, Liu VX, Iwashyna TJ, Brunkhorst FM, Rea TD, Scherag A, Rubenfeld G, Kahn JM, Shankar-Hari M, Singer M, Deutschman CS,

Escobar GJ, Angus DC. Assessment of clinical criteria for sepsis: for the third international consensus definitions for sepsis and septic shock (Sepsis-3). JAMA 2016; 315: 762-774.

[7] Manzoli TF, Troster EJ, Ferranti JF, Sales MM. Prolonged suppression of monocytic human leukocyte antigen-DR expression correlates with mortality in pediatric septic patients in a pediatric tertiary Intensive Care Unit. J Crit Care 2016; 33: 84-89.

[8] Singer M, Deutschman CS, Seymour CW, Shankar-Hari M, Annane D, Bauer M, Bellomo R, Bernard GR, Chiche JD, Coopersmith CM, Hotchkiss RS, Levy MM, Marshall JC, Martin GS, Opal SM, Rubenfeld GD, van der Poll T, Vincent JL, Angus DC. The third international consensus definitions for sepsis and septic shock (Sepsis-3). JAMA 2016; 315: 801-810.

[9] Hotchkiss RS, Karl IE. The pathophysiology and treatment of sepsis. N Engl J Med 2003; 348: 138-150.

[10] Rhodes A, Evans LE, Alhazzani W, Levy MM, Antonelli M, Ferrer R, Kumar A, Sevransky JE, Sprung CL, Nunnally ME, Rochwerg B, Rubenfeld GD, Angus DC, Annane D, Beale RJ, Bellinghan GJ, Bernard GR, Chiche JD, Coopersmith C, De Backer DP, French CJ, Fujishima S, Gerlach H, Hidalgo JL, Hollenberg SM, Jones AE, Karnad DR, Kleinpell RM, Koh Y, Lisboa TC, Machado FR, Marini JJ, Marshall JC, Mazuski JE, McIntyre LA, McLean AS, Mehta S, Moreno RP, Myburgh J, Navalesi P, Nishida O, Osborn TM, Perner A, Plunkett CM, Ranieri M, Schorr CA, Seckel MA, Seymour CW, Shieh L, Shukri KA, Simpson SQ, Singer M, Thompson BT, Townsend SR, Van der Poll T, Vincent JL, Wiersinga WJ, Zimmerman JL, Dellinger RP. Surviving sepsis campaign: international guidelines for management of sepsis and septic shock: 2016. Intensive Care Med 2017; 43: 304-377.

[11] Sung PH, Chiang HJ, Chen CH, Chen YL, Huang TH, Zhen YY, Chang MW, Liu CF, Chung SY, Chen YL, Chai HT, Sun CK, Yip HK. Combined therapy with adipose-derived mesenchymal stem cells and ciprofloxacin against acute urogenital organ damage in rat sepsis syndrome induced by intrapelvic injection of cecal bacteria. Stem Cells Transl Med 2016; 5: 782-792.

[12] Chang CL, Sung PH, Chen KH, Shao PL, Yang CC, Cheng BC, Lin KC, Chen CH, Chai HT, Chang HW, Yip HK, Chen HH. Adipose-derived mesenchymal stem cell-derived exosomes alleviate overwhelming systemic inflammatory reaction and organ damage and improve outcome in rat sepsis syndrome. Am J Transl Res 2018; 10: 1053-1070.

[13] Bolton CF, Young GB, Zochodne DW. The neurological complications of sepsis. Ann Neurol 1993; 33: 94-100.

[14] Hund E. Neurological complications of sepsis: critical illness polyneuropathy and myopathy. J Neurol 2001; 248: 929-934.

[15] Wratten ML. Therapeutic approaches to reduce systemic inflammation in septic-associated neurologic complications. Eur J Anaesthesiol Suppl 2008; 42: 1-7.

[16] Hocker SE, Wijdicks EF. Neurologic complications of sepsis. Continuum (Minneap Minn) 2014; 20: 598-613.

[17] Schmutzhard E, Pfausler B. Neurologic complications of sepsis. Handb Clin Neurol 2017; 141: 675-683.

[18] Cronshaw HL, Daniels R, Bleetman A, Joynes E, Sheils M. Impact of the Surviving Sepsis Campaign on the recognition and management of severe sepsis in the emergency department: are we failing? Emerg Med J 2011; 28: 670-675.

[19] Hein F, Massin F, Cravoisy-Popovic A, Barraud D, Levy B, Bollaert PE, Gibot S. The relationship between CD4+CD25+CD127- regulatory T cells and inflammatory response and outcome during shock states. Crit Care 2010; 14: R19.

[20] Taylor AL, Llewelyn MJ. Superantigen-induced proliferation of human CD4+CD25- T cells is followed by a switch to a functional regulatory phenotype. J Immunol 2010; 185: 6591-6598.

[21] Venet F, Chung CS, Monneret G, Huang X, Horner B, Garber M, Ayala A. Regulatory T cell populations in sepsis and trauma. J Leukoc Biol 2008; 83: 523-535.

[22] Venet F, Chung CS, Kherouf H, Geeraert A, Malcus C, Poitevin F, Bohe J, Lepape A, Ayala A, Monneret G. Increased circulating regulatory T cells (CD4(+)CD25 (+)CD127 (-)) contribute to lymphocyte anergy in septic shock patients. Intensive Care Med 2009; 35: 678-686.

[23] Chen HH, Lai PF, Lan YF, Cheng CF, Zhong WB, Lin YF, Chen TW, Lin H. Exosomal ATF3 RNA attenuates pro-inflammatory gene MCP-1 transcription in renal ischemia-reperfusion. J Cell Physiol 2014; 229: 1202-1211.

[24] Chen KH, Chen CH, Wallace CG, Yuen CM, Kao GS, Chen YL, Shao PL, Chen YL, Chai HT, Lin KC, Liu CF, Chang HW, Lee MS, Yip HK. Intravenous administration of xenogenic adipose-derived mesenchymal stem cells (ADMSC) and ADMSC-derived exosomes markedly reduced brain infarct volume and preserved neurological function in rat after acute ischemic stroke. Oncotarget 2016; 7: 74537-74556.

[25] Fleig SV, Humphreys BD. Rationale of mesenchymal stem cell therapy in kidney injury. Nephron Clin Pract 2014; 127: 75-80.

[26] Ko SF, Yip HK, Zhen YY, Lee CC, Lee CC, Huang CC, Ng SH, Lin JW. Adipose-derived mesenchymal stem cell exosomes suppress hepatocel-

lular carcinoma growth in a rat model: apparent diffusion coefficient, natural killer t-cell responses, and histopathological features. Stem Cells Int 2015; 2015: 853506.

[27] Zhou Y, Xu H, Xu W, Wang B, Wu H, Tao Y, Zhang B, Wang M, Mao F, Yan Y, Gao S, Gu H, Zhu W, Qian H. Exosomes released by human umbilical cord mesenchymal stem cells protect against cisplatin-induced renal oxidative stress and apoptosis in vivo and in vitro. Stem Cell Res Ther 2013; 4: 34.

[28] Zou X, Zhang G, Cheng Z, Yin D, Du T, Ju G, Miao S, Liu G, Lu M, Zhu Y. Microvesicles derived from human Wharton's Jelly mesenchymal stromal cells ameliorate renal ischemia-reperfusion injury in rats by suppressing CX3CL1. Stem Cell Res Ther 2014; 5: 40.

[29] Lin KC, Yip HK, Shao PL, Wu SC, Chen KH, Chen YT, Yang CC, Sun CK, Kao GS, Chen SY, Chai HT, Chang CL, Chen CH, Lee MS. Combination of adipose-derived mesenchymal stem cells (ADMSC) and ADMSC-derived exosomes for protecting kidney from acute ischemia-reperfusion injury. Int J Cardiol 2016; 216: 173-185.

[30] Sun CK, Chen CH, Chang CL, Chiang HJ, Sung PH, Chen KH, Chen YL, Chen SY, Kao GS, Chang HW, Lee MS, Yip HK. Melatonin treatment enhances therapeutic effects of exosomes against acute liver ischemia-reperfusion injury. Am J Transl Res 2017; 9: 1543-1560.

[31] Day YJ, Chen KH, Chen YL, Huang TH, Sung PH, Lee FY, Chen CH, Chai HT, Yin TC, Chiang HJ, Chung SY, Chang HW, Yip HK. Preactivated and disaggregated shape-changed platelets protected against acute respiratory distress syndrome complicated by sepsis through inflammation suppression. Shock 2016; 46: 575-586.

[32] Chen YT, Yang CC, Shao PL, Huang CR, Yip HK. Melatonin-mediated downregulation of ZNF746 suppresses bladder tumorigenesis mainly through inhibiting the AKT-MMP-9 signaling pathway. J Pineal Res 2019; 66: e12536.

[33] Sung PH, Lee FY, Lin LC, Chen KH, Lin HS, Shao PL, Li YC, Chen YL, Lin KC, Yuen CM, Chang HW, Lee MS, Yip HK. Melatonin attenuated brain death tissue extract-induced cardiac damage by suppressing DAMP signaling. Oncotarget 2018; 9: 3531-3548.

C NF-κB

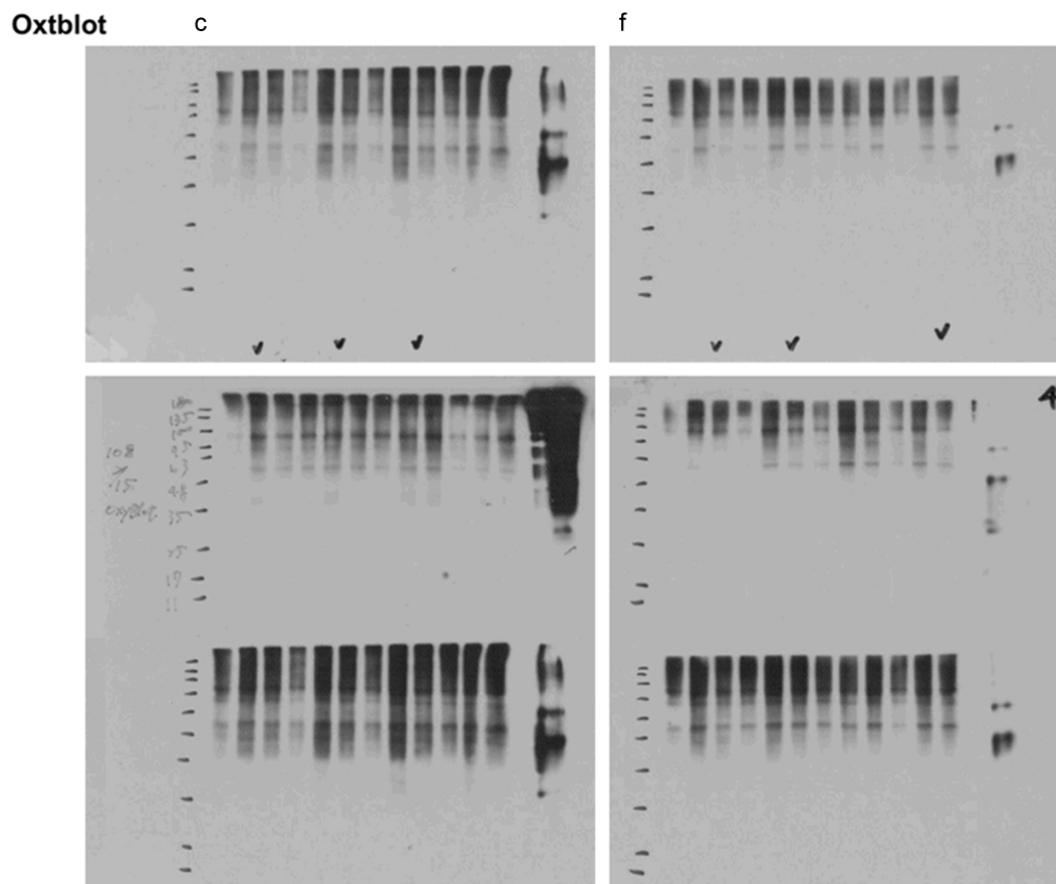MMP-9

IL-1β

TNF-α

D NOX-1

NOX-2

2
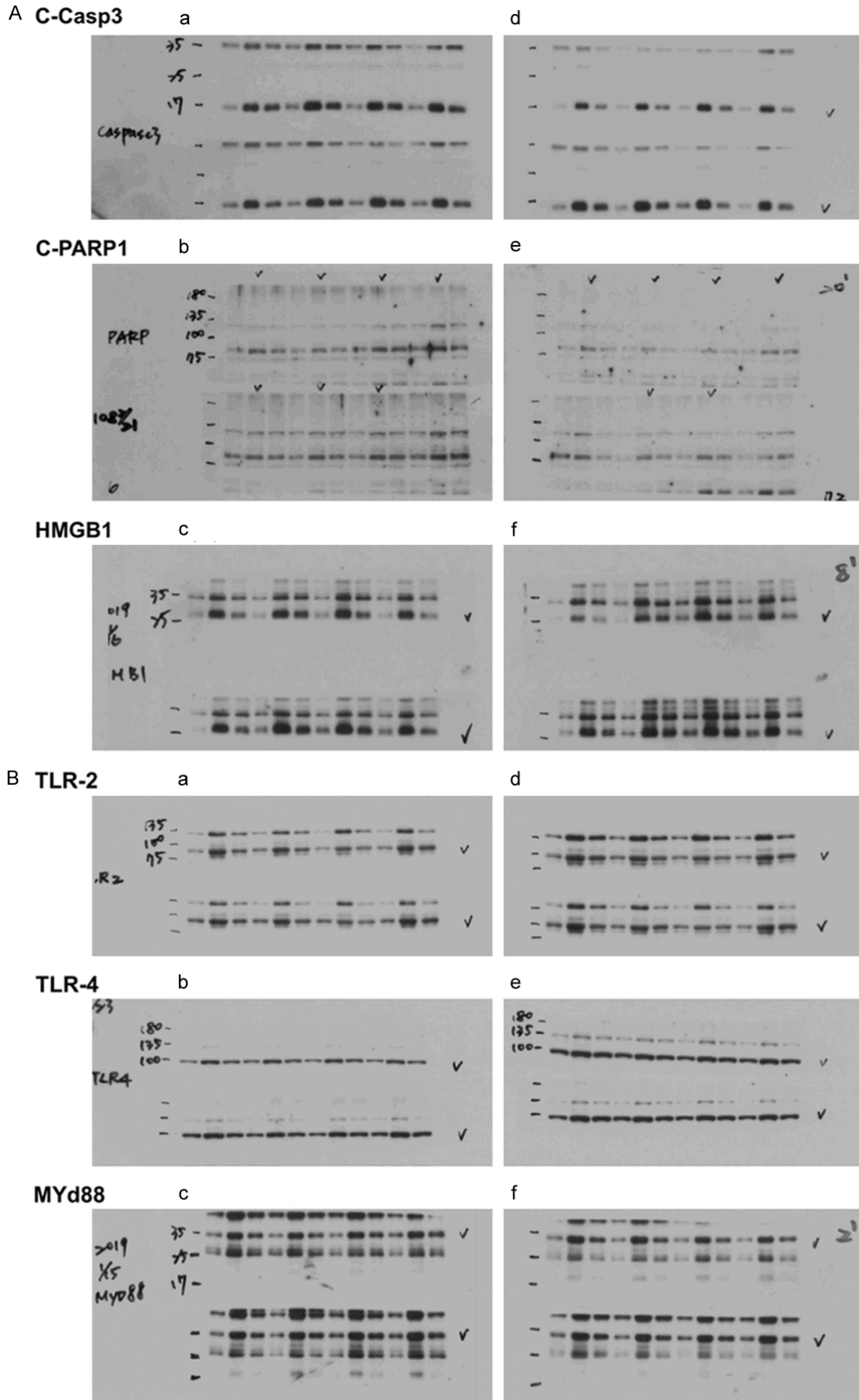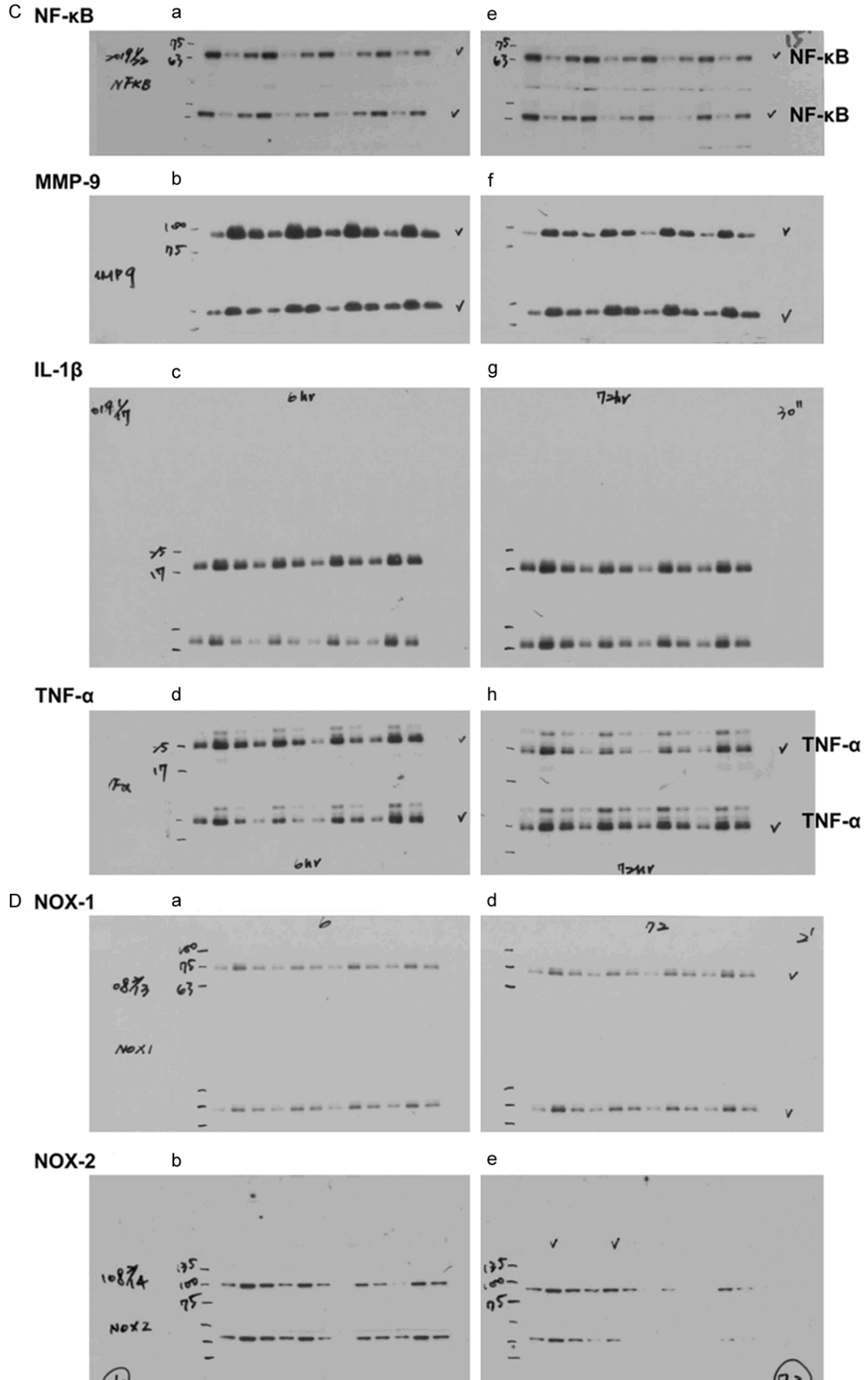
Figure S1. A-D. Illustrating the raw materials of Western blotting (i.e., including the whole films/membranes).